ROBUST STABILIZATION OF DC-DC BUCK CONVERTER VIA BOND-GRAPH PROTOTYPING

[a]Sergio Junco, [b]Juan Tomassini, [c]Matías Nacusse

[a],[b],[c]LAC, Laboratorio de Automatización y Control, Departamento de Control, Escuela de Ingeniería Electrónica, Facultad de Ciencias Exactas e Ingeniería, Universidad Nacional de Rosario, Argentina

[a]sjunco@fceia.unr.edu.ar, [b]tomajuan@fceia.unr.edu.ar, [c]nacusse@fceia.unr.edu.ar

ABSTRACT

This paper presents the application of a technique called Bond-Graph Prototyping (BGP) to the design of a robust controller globally stabilizing an arbitrary equilibrium point of the DC-DC Buck converter. The method qualifies as an energy- and power-based design, as it proceeds entirely in the BG domain. The nonlinear averaged BG of the converter is used as the plant model. The first design step is to construct a so-called Target BG (TBG) specifying the desired closed-loop behaviour. Then, via BGP, a Virtual BG emulating the internal behaviour of the modulated source providing the control action is constructed which, coupled to the plant BG yields an equivalent to the TBG. Finally, integral action is applied to the closed-loop in order to provide robustness against parameter uncertainty and external disturbances. The design is performed for a generic dissipative load and then particularized for a linear resistance, for which the numerical validation via simulation is provided.

Keywords: Buck converter, bond graphs, energy-based controller design, robust integral control, structure-preserving control.

1. INTRODUCTION

Due to their versatility, high efficiency, controllable behaviour, fast dynamics and wide-range of power management, Power Electronic Converters (PEC) are ubiquitous and pervade most of the cutting-edge engineering application areas. Indeed, they can be found in electrical drives, switched-mode power supplies, battery chargers, uninterrupted power supplies, all type of mobile devices, distributed generation and renewable energy conversion systems, embedded in electric/hybrid vehicles (cars, trains and airplanes), etc. (F. Dong Tan 2013).

Closed-loop control of PEC is mandatory when their mission is the conditioning of the processed or the output power subject to hard application specifications and under the effect of significant disturbances. Model-based control system synthesis methods are required for high-performance behaviour, see for instance (Bacha, Munteanu and Bratcu 2014). Through its application to the control of a buck converter, this paper presents a method to address these kind of problems in the Bond Graph domain (Karnopp, Margolis & Rosenberg, 2012). From a modelling perspective, PEC are hybrid, non linear systems composed of continuous elements like inductors, capacitors, resistors, sources, etc., and switching devices allowing for the control actions, like transistors, diodes, etc. Considering the controller outputs as logic variables determining directly the on-off states of the switches, or as continuous variables acting on them through PWM stages, establishes a major divide between the design strategies. To the first case belongs, for instance, the sliding-mode approach (Tan, Lai, Tse and Cheung 2006), to the second, the vast majority of techniques, which develop on a averaged continuous model. Aiming at its implementation on a digital processor, the control algorithm can be obtained as a continuous-time law that needs further discretization or directly as a discrete-time law on a discretized average model (Choudhury 2005). A further division concerns the direct use of nonlinear averaged models or their versions linearized around a desired equilibrium point (Bacha, Munteanu and Bratcu 2014). Linear controllers are tuned for specific operating points and, unless complemented with adaptation mechanisms –what adds complexity to the controller–,the closed-loop performance degrades when the operating point changes. Nonlinear controllers with a unique parameterization valid for the whole operating range are thus preferable. Exact feedback-linearization, passivity-based control and Lyapunov-like stabilization count among the continuous time control techniques derived on nonlinear averaged continuous converter models (Sira-Ramírez and Silva-Ortigoza 2006).

This paper presents the Bond Graph Prototyping technique (Junco 2004) as applied to the nonlinear averaged Bond Graph model of a buck converter. In this context, BGP means constructing a Virtual BG (VBG) that, when coupled to the plant at the place of the actuator, produces a desired closed-loop behaviour having been pre-specified in the form of a Target BG (TBG) whose storage function qualifies as a Lyapunov function, so that the closed-loop stability is assured. In the case of the averaged model of the buck converter the

actuator is a voltage source modulated by the duty-cycle of the switching control signal, that can be also modelled as a MTF supplied by the a source, as done here in Figure 1. The resultant controller is a nonlinear static feedback law dependent on the plant parameters. As such it is strongly sensitive to parameter deviations and external disturbances, what calls for a secondary robustifying control loop, which is designed adding integral action in such a way that the closed-loop stability is guaranteed.

The purpose of the paper is twofold: on the one hand, to present the BG-based control system design methodology as applied to PEC applications and, collaterally, to contribute a new result specific for the buck converter. As it proceeds entirely in the BG domain, the method qualifies as an energy- and power-based design. For this reason there is an intrinsic correspondence with the energy-shaping and interconnection-and-damping assignment techniques (ES and IDA) developed on Port-Hamiltonian models (PHS), particularly with the SIDA-PBC (Simultaneous Energy Shaping and Damping Assignment) approach (Batlle, Dòria-Cerezo, Espinosa-Pérez and Ortega, 2009), as shown in the paper. Furthermore, as the TBG is chosen to be linear, the result is equivalent to designing with the feedback-linearization technique (Khalil 2002). It is however important to remark that this is not inherent to the method but a consequence of having made the particular choice of a linear closed-loop behaviour.

The remainder of the paper is organized as follows: Section 2 presents the averaged BG-model of the buck converter, develops the basic control law via BG-prototyping assuming perfect model knowledge, establishes the closed-loop properties and shows via simulation the shortcomings of the controller under the presence of model uncertainties. Also the correspondence of the result with controllers obtained via IDA-PBC and feedback-linearization is shown in this section. Section 3 deals with the BG-based design of an additional integral control action that preserves the closed-loop PHS-structure and rejects internal and external disturbances. The behaviour of the robustified overall control law is demonstrated in this section with the help of simulation results. The paper ends with Section 4 presenting the conclusions.

2. FULL STATE-FEEDBACK CONTROLLER FOR EXACT MODEL KNOWLEDGE

This section presents the averaged BG model of the buck converter, formulates the control problem in terms of equivalent closed-loop stored energy and power dissipation by means of the TBG, and solves it with resource to the BGP method. Furthermore, the performance of the controller by exact model knowledge is shown by simulations, as well as its degradation under the presence of disturbances.

2.1. Buck converter averaged model

Figure 1a shows the equivalent circuit of a buck converter with a generic load specified by a nonlinear law $i_L = h(v)$ satisfying $v . h(v) > 0$ for $v > 0$ and $h(v) = 0$ for $v = 0$, i.e., entirely contained in the first and third quadrant thus being truly dissipative. Figure 1b shows the averaged BG of the equivalent circuit where the commutation cell constituted by the switch (a MOSFET or IGBT in the practice) and the diode has been replaced by the source-supplied MTF driven by $d(t)$, the continuously varying duty cycle of the commutation signal controlling the switch, see Mohan, Undeland, and Robbins (1995) for background on averaged models. In the calculations to follow $u = d\,E$, the averaged voltage across the diode, will be treated as the control input.
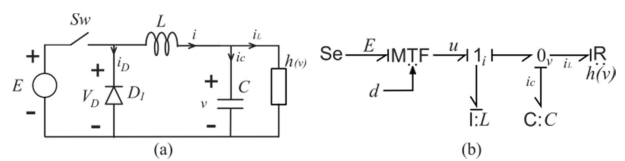

Figure 1: Buck converter: (a) Equivalent circuit. (b) Averaged BG model.

The averaged state equations are:

$$\frac{di}{dt} = -\frac{v}{L} + \frac{u}{L}$$
$$\frac{dv}{dt} = \frac{i}{C} - \frac{h(v)}{C} \tag{1}$$

Here, instead of the inductance magnetic flux and capacitor electric charge, the p and q energy variables usually chosen as state variables in the BG domain, their power co-variables i and v have been selected. This is because they are more frequently used in the power electronics literature.

With the duty cycle taken values in the interval [0, 1] and assuming the converter operating in continuous conduction mode (CCM), the following mathematical restrictions apply:

$$i > 0$$
$$v \geq 0 \tag{2}$$

A generic equilibrium point (EP) is defined by $(\bar{v}, \bar{i}) = (V, I)$, where V is a desired constant output voltage on the load and I is the corresponding current given by $I = h(V)$.

2.2. BG-prototyping the control law

The control problem is to render a desired EP (V, I) globally asymptotically stable (GAS), i.e., to find a controller that forces all the trajectories starting in the first quadrant –recall restriction (2)– to remain there, be bounded and to converge to the EP.

2.2.1. Target Bond Graph

The first step in the control system synthesis procedure consists in expressing the desired closed-loop behaviour

in the form of a BG, what originates the concept of Target Bond Graph. This TBG is conveniently defined or chosen as an autonomous system having its origin as a GAS EP in a one-to-one correspondence with the desired EP of the converter. The chosen TGB is given in Figure 2 along with its electric circuit equivalent. It is an inputless system with two linear storage components (their parameters have been chosen equal to the original L and C parameters, but it could have been done differently) and two linear dissipators (whose parameters are the resistance R and conductance G) each one being driven by a state variable. Thus, the TBG has the state space origin as its only EP which, clearly, is GAS. In fact, more than that, due to the TBG linearity and invariance, the EP is GES, globally exponentially stable. This can be seen directly by inspection of the TBG (Junco 2001a, Proposition 2.3) or noticing that the stored energy W is a positive definite function (written > 0) with negative definite (< 0) orbital derivative $\dot{W}$ thus qualifying as a Lyapunov function for the origin, see equations (3) and (4).
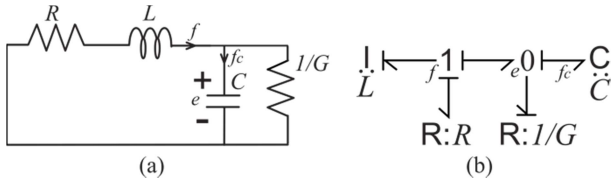

Figure 2: (a) Target BG. (b) Equivalent Circuit.

$$W(e,f) = \tfrac{1}{2}Ce^2 + \tfrac{1}{2}Lf^2 > 0 \tag{3}$$

$$\dot{W}(e,f) = -Ge^2 - Rf^2 < 0 \tag{4}$$

The capacitor C in the TBG is taken as being the original one but with its voltage e referred to the desired value V, so that the following relationships hold

$$e = v - V \tag{5}$$
$$f_C = i_C \tag{6}$$

where f_C and i_C are the currents flowing into the capacitors of the TBG and the Plant-BG, respectively. On the other hand, the currents i_C in the Plant-BG and f in the TBG do satisfy

$$i_C = i - h(v) \tag{7}$$
$$f = f_C + G\,e \tag{8}$$

Putting all together yields the next correspondences between the variables of the Plant-BG and the TGB:

$$\begin{aligned} v &= e + V \\ i &= f + h(e + V) - Ge \end{aligned} \tag{9}$$

The change of variables (9) clearly shows the following correspondence between the EPs:

$$(\bar{v}, \bar{\iota}) = (V, I) \Leftrightarrow \{e = 0 \wedge f = 0\} \tag{10}$$

Proposition 1: The EP (V, I) of the converter in closed-loop with a (well-defined) control law enforcing the change of variables (9) is GAS.

Proof. The GES-property of $(e = 0, f = 0)$ determined by (3) and (4) implies that the trajectories $(e(t), f(t))$ are bounded and converge to the origin. Then, because of (9) the trajectories $(v(t), i(t))$ are also bounded and converge asymptotically to (V, I).

What remains left to solve the problem is to find the control law enforcing a closed-loop behaviour equivalent to the behaviour of the TBG, i.e., enforcing the satisfaction of the change of variables (9) and the GES of the EP $(e = 0, f = 0)$. This is done in the sequel via BG-Prototyping.

2.2.2. Virtual Bond Graph
The BGP technique consists basically in constructing a Virtual BG (Junco 2004) that, replacing the ensemble {effort-source + MTF} in Figure 1b, and exchanging power with the rest of the system, will produce the necessary control signal u in order for the interconnected system to exactly emulate the behaviour of the TBG. This procedure is illustrated following four steps with the help of Figure 3.
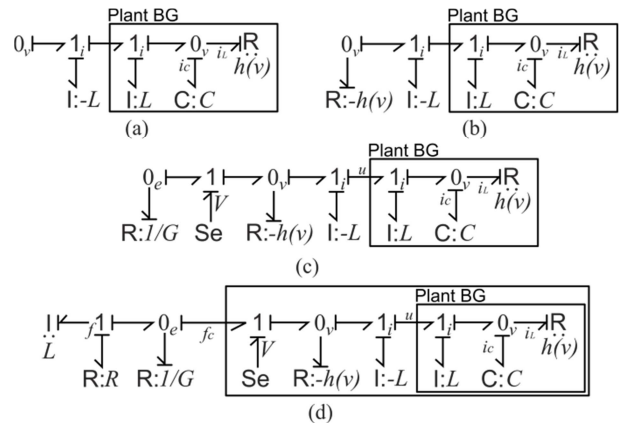

Figure 3: Construction of Virtual BG. Step 1 (a), step 2 (b), step 3 (c) and step 4 (d).

In the TBG there is a linear dissipator (conductance G) instead of the original nonlinear load (NLL) in parallel with the C-element. Achieving this demands first cancelling the NLL (inserting a R-element with its flow being the opposite of the NLL-flow, i.e. $flow = -h(v)$ and then assigning the linear dissipator to a 0-junction with a common effort e, that has to be created. Finally, the aggregate of the I and R elements appearing in the TBG as sharing the common flow f must be added.

To do this in the VBG it is necessary first to gain access (meaning to reproduce inside it) the 0-junction where the {C+NLL} parallel is connected. This is done in the first prototyping step (Figure 3a) adding the element $I : -L$ that cancels the (effect of the) inductance L. Note that derivative causality have been assigned on purpose to both inertias in order to easily show the reproduction of the effort v in the 0-junction of the

VBG. The second step (Figure 3b) cancels the original NLL. The construction of the 0-junction with the effort e and the assignment of the linear dissipation is shown in the third step (Figure 3c). The fourth and final step, shown in Figure 3d, completes the prototyping of the control law via the addition of the series-connected I and R.

Remark that the presence of the resistance R in the TBG is not necessary in order to achieve exponential stability. In fact, (3) and (4) with R = 0 in (4) allow to conclude the Lyapunov stability of the EP which, complemented with Lasalle's Invariance Theorem proves the exponential stability. However it is convenient to include this resistence as its parameter provides one more degree of freedom to the controller (the other being the value G of the conductance) to impose a desired closed-loop performance.

Some elementary algebra on the junctions of Figure 3d immediately shows that the part of the BG framed by a rectangular box is equivalent to a capacitor working at a voltage e and draining a current i_C, i.e., satisfying (5), (6), and exactly equivalent to the C-element of the TBG.

The state feedback control law given in (11) is easily calculated starting on the BG of Figure 3d as follows: first, read the control variable u on the Plant BG via the standard equation formulation procedure and, second, use the change of variables (9) to put the resulting expression in terms of the system state variables. Notice the appearance of $h'(v) := \frac{dh(v)}{dv}$, the incremental conductance associated to the NLL, through the time derivative of the inductance current.

$$u = -RG\,v + V\,(1 + RG) + (i - h(v))\left(\frac{L}{C}h'(v) - R - \frac{L}{C}G\right) \tag{11}$$

The duty cycle d, the true control input, can be immediately calculated as $d = u/E$.

Using the change of variables (9) it can be easily checked that replacing (11) in (1) yields a closed-loop dynamics equivalent to the dynamics of the TBG of Figure 2. The above properties are summarized next.

2.3. Properties of the control law
The control law (11) in closed-loop with system (1):

1. Globally asymptotically stabilizes its EP $(\bar{v}, \bar{\imath}) = (V, I)$. "Globally" refers here to the domain of definition of the problem, see restrictions (2).

2. Establishes the relationships (9) among the variables of the closed-loop system and the TBG, which in turn determines the equivalence between both of them with the following properties:

   i) The following one-to-one correspondence between the EP of both systems holds:
   $$(\bar{e}, \bar{f}) = (0,0) \leftrightarrow (\bar{v}, \bar{\imath}) = (V, I)$$

   ii) The mathematical restrictions (2) on (v, i) imply the following restrictions on (e, f):

$$e \geq -V$$
$$f > Ge - h(e + V) \tag{12}$$

Remark. The state-space origin $(\bar{e}, \bar{f}) = (0,0)$ of the TBG *per se* is GES, with the complete state space (the $(\bar{e}, \bar{f})$-plane) being is domain of attraction. But the TBG being tied to system (1) by (9) determines the reduction of this domain to (12).

2.4. Equivalence with other control methods
Having specified the closed-loop behaviour as a TBG, which is clearly equivalent to a PHS, this method is inherently comparable to the ES-and-IDA technique of the PBC approach to control of nonlinear physical systems. As the TBG *simultaneously* specifies the closed-loop storage and dissipation functions, it corresponds to the particular method called SPBC, where S stands for Simultaneous (Batlle, Dòria-Cerezo, Espinosa-Pérez and Ortega, 2009). On the other hand, as the TBG is a LTI-system, deriving the controller with the BG-Prototyping method must be equivalent to doing it applying the exact-feedback linearization technique (Khalil 2002). This is not inherent to the method but just a consequence of the particular choice of a LTI-TBG to represent the closed-loop system. The details of both equivalences are given next.

2.4.1. Energy Shaping and IDA-PBC
The IDA-PBC method assigns both a storage and a dissipation function to the closed-loop. In this specific case, the Hamiltonians (storage functions) in closed-loop $H(v, i)$ and open-loop $H_{OL}(v, i)$ are related by:

$$H(v, i) = H_{OL}(v, i) + H_a(v, i) \tag{13}$$

Where H_a is the energy added by the controller in order for $H(v, i)$ to have its minimum at the EP (V, I) and, in certain cases (as in this one), being a Lyapunov function of (v, i); for a rigorous formulation of this method see, for instance, (Ortega, van der Schaft, Maschke, and Escobar 2002).

The Hamiltonians H and H_a induced by the method developed in the previous section are calculated next. Due to the equivalence between the TBG and the closed-loop system, the function H equals the storage function (3) associated to the TBG but written in terms of the original variables (v, i), as shown below:

$$W(e, f) = \tfrac{1}{2}Ce^2 + \tfrac{1}{2}Lf^2 \tag{3}$$

$$H(v, i) = W\big(e(v), f(v, i)\big) = \frac{i^2 L}{2} + \frac{Cv^2}{2} + \frac{h^2(v)\,L}{2} - h(v)i\,L - Gh(v)L\,v + GiLv + \tfrac{1}{2}G^2Lv^2 + Gh(v)LV - GiLV - CvV - G^2LvV + \frac{Cv^2}{2} + \tfrac{1}{2}G^2LV^2 \tag{14}$$

The sum of the first two terms on the right side of (14) equals the open-loop Hamiltonian:

$$H_{OL}(v, i) = \tfrac{1}{2}\,L\,i^2 + \tfrac{1}{2}\,C\,v^2 \tag{15}$$

It is concluded then that the energy $H_a(v,i)$ added by the controller is:

$$H_a(v,i) = \frac{h^2(v)\,L}{2} - h(v)i\,L - Gh(v)L\,v + GiLv +$$
$$\frac{1}{2}G^2Lv^2 + Gh(v)LV - GiLV - CvV - G^2LvV + \frac{CV^2}{2} +$$
$$\frac{1}{2}G^2LV^2 \qquad (16)$$

The control parameters R and G have the physical interpretation of a resistance in series with the inductance and a conductance in parallel with the capacitor. Thus, they are equivalent to a closed-loop damping that can be characterized by the rate at which they diminish the stored energy, which is simply stated in (4). The damping added by the controller can be calculated writing the right hand side of (4) in terms of v and i and substracting from this expression the open loop damping, i.e., the product $v.h(v)$.

2.4.2. Exact-feedback linearization

Following the standard design procedure for I/O exact feedback linearization (Khalil 2002) leads to the following control law, with the capacitor voltage v being chosen as output:

$$u = LC\left[\frac{1}{LC}v + \frac{1}{C^2}ih'(v) - \frac{1}{C^2}h(v)h'(v) - K_1\dot{v} -\right.$$
$$\left. K_2(v - V)\right] \qquad (17)$$

The parameters K_1 and K_2 are positive free gains. The following choice of them makes the control law (17) equivalent to the one specified in (11):

$$K_1 = \frac{G}{C} + \frac{R}{L}$$
$$K_2 = \frac{1}{LC}(1 + RG) \qquad (18)$$

2.5. Analysis of the ideal control law via simulation

In this subsection some simulations results are presented to show the performance of the control law (11) with a linear resistive load i.e. $h(v) = v/R_L$. First the control law is tested under perfect knowledge of the model parameters and secondly with parameter dispersion in some key electrical components, as the voltage source and the load resistance.

The parameters used in the simulations are: $L = 500\mu H$, $C = 1000\mu F$, $R_L = 20\Omega$, $E = 22.2V$, $R = 1.5\Omega$ and $G = 0.05\,\Omega^{-1}$. This set of parameters is used in (Kwasinski and Krein 2007) for a constant power load, here a linear load resistance is used.

2.5.1. Complete knowledge of parameters and load

Figures 4 (a) and (b) show the phase portraits of the closed loop system with voltage references $V = 13,5V$ and $V = 18V$, respectively, for different initial conditions.

The next experiment, whose time responses are used to evaluate the performance of the closed loop system, is designed as follows:

Experiment 1: the system starts with zero initial conditions and the voltage reference is set at $V = 18V$. Later, at time $t = 20ms$ the voltage reference changes to $V = 16.7V$.

Figure 5 shows the time response of the current (i), duty cycle (d), output voltage (v) and voltage error (e). Notice that the closed loop system works as a linear system, since the duty cycle is less than one and the circuit is always in CCM.

Figure 6 show the state space response of *Experiment 1*, where the red stars represent the equilibrium points for each reference voltage.
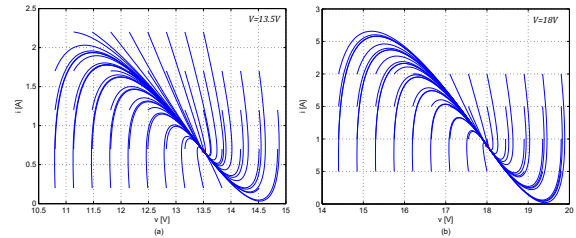

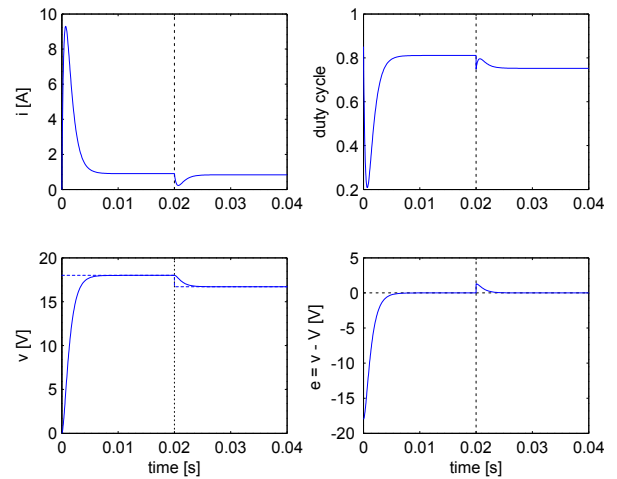Figure 4: Phase portrait with linear resistive load for reference voltage (a) $V = 13,5V$ and (b) $V = 18V$.
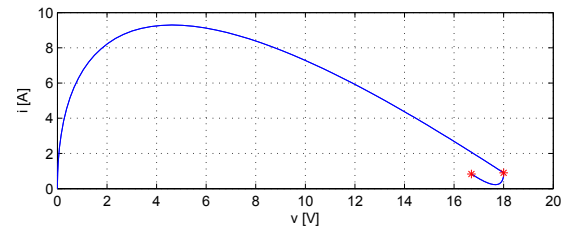

Figure 5: Time responses of Experiment 1.

Figure 6: State space trajectory for Experiment 1.

2.5.2. Performance degradation under parameter uncertainties

Figures 7 and 8 show the simulation results of *Experiment 1* with plant parameters $R_L = 24\Omega$ and $E = 19.98V$. Recall that the controller uses the values $R_L = 20\Omega$ and $E = 22.2V$.
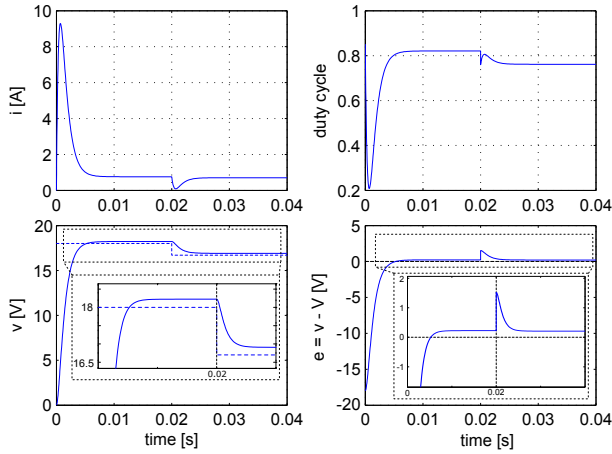
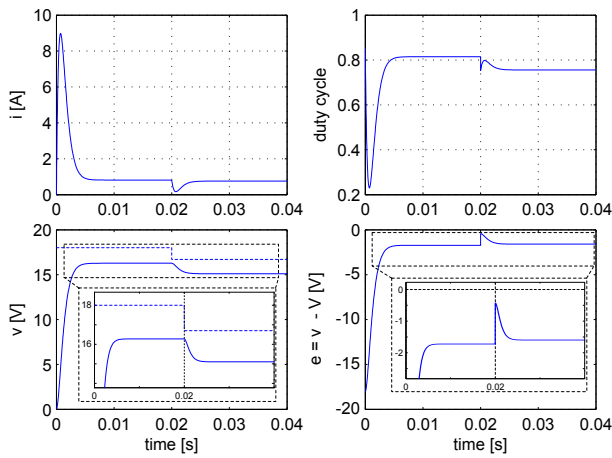Figure 7: Simulation response with $R_L = 24\Omega$

Figure 8: Simulation response with $E = 19.98V$

Looking at the zoomed-in inserts in the figures of the voltage and its error it can be noticed that in both cases, the output voltage v does not reach its reference value. This is due to the fact that the procedure used to obtain (11) is based on the complete knowledge of the system parameters and load. Figure 7 shows that a slight variation in the load resistance (R_L) implies that applying (11) in (1) no longer yields the desired target circuit. This results in a steady state error $e \neq 0$. In Figure 8, recalling $d = u/E$, if the DC link voltage is not measured (and supposed constant) then the duty cycle is miscalculated, resulting again in a steady state error and $e \neq 0$.

3. ROBUSTIFICATION OF THE CONTROL LAW

Involving multiple cancellations, the procedure developed in the previous section produces a control law dependent on the plant parameters L, C and V, and the load-related functions $h(v)$ and $h'(v)$ (the dependence of both reduced to R_L in the simulation example). As shown by the simulation outcomes of the last subsection, the lack of exact knowledge of these data results in the degradation of the closed-loop performance. In a real application it is necessary to

robustify the control law (11) against parameter dispersions and some external disturbances in order to fulfill the control objectives, i.e., regulation of the output voltage, even under their presence. This task is carried out next by adding an outer control loop. Thus, the control input is defined as:

$$u = u_i + u_o, \tag{19}$$

Where u_i is the control law (11) and u_o will be designed to reject the disturbances. Consider the perturbed plant:

$$\frac{di}{dt} = -\frac{v}{L} + \frac{u}{L} + \delta_1$$
$$\frac{dv}{dt} = \frac{i}{C} - \frac{h(v)}{C} + \delta_2 \tag{20}$$

Where δ_1 and δ_2 can be state dependent disturbances, due to parameter dispersion, unmodelled dynamics, or external disturbances. Replacing (19) and (11) into (20) and using (9) yields the perturbed closed-loop system:

$$\frac{df}{dt} = -\frac{R}{L}f - \frac{1}{L}e + \frac{1}{L}u_o + \tilde{\delta}_1$$
$$\frac{de}{dt} = \frac{1}{C}f - \frac{G}{C}e + \tilde{\delta}_2 \tag{21}$$

Where $\tilde{\delta}_1 = \delta_1/L + \frac{1}{C}\delta_2(G - h'(v))$ and $\tilde{\delta}_2 = \delta_2/C$. Notice that the perturbed closed-loop equations are expressed in the states variables of the TBG. The perturbed TBG is shown on the right side on Fig. 9.

3.1. Integral control action

The traditional technique to robustify a control law against parameter dispersion and to simultaneously reject disturbances is to provide integral action (IA) through an additional control loop (Khalil 2002). To the extent of our knowledge, the first ideas to solve these problems on BGs have been presented in (Junco 2001a). Later on, the ideas of TBG and VBG, formally presented in (Junco 2004), were used in (Donaire and Junco 2009a) to enhance a controller designed in the BG-domain with a structure-preserving IA, and further generalized in (Donaire and Junco 2009b) to the framework of passivity-based control on PHS-models in order to add IA *on non-passive outputs*, i.e., outputs with relative degree equal to or greater than two with respect to the control input. It is stressed that the method for adding integral action on the *passive* outputs of PHS models was first presented in (Ortega and García-Canseco 2004).

Applying again the BGP-technique, the VBG of Figure 9 is constructed, where the control input, i.e., the IA on the variable e, is obtained next via the same procedure detailed in Section 2. It can be seen that the 0-junction with associated effort e is reproduced in the VBG via BGP, and that an I-element is attached to it. Precisely this element performs the disturbance-rejecting IA: any deviation from zero of the capacitor voltage e generates a current f_{IA} (which is chosen as the state variable) in

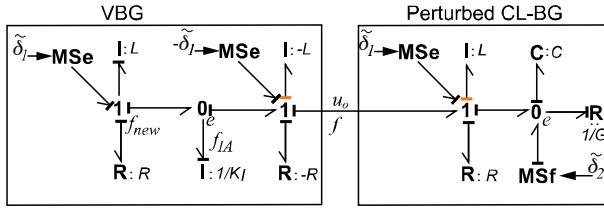the inertia that is fed into the capacitor until the voltage falls again to zero.

Figure 9: BG of the perturbed CL (right) and VBG.

Notice that to access the effort e, the effect of $\tilde{\delta}_1$, acting on the 1-junction with common flow equal to f, has been cancelled in the VBG of Figure 9. This action does not imply the knowledge of the disturbance $\tilde{\delta}_1$ – which in general cannot be measured – to define the control law u_o because its effect has been compensated in the new 1-junction with common flow f_{new}. This result in a control law u_o that depends only on the variable e. Thus, at the level of the outer control signal u_o, the effect of adding this I-element translates into the PI-law given in (22):

$$u_o = \frac{L}{K_I} e + \frac{R}{K_I} \int e \qquad (22)$$

This control action generates the new closed-loop BG model shown in Figure 10. Notice that the IA implies a dynamic extension of the controller that increases the order of the closed-loop system to 3 through the new state variable f_{IA}. Also notice that the new TBG of Figure 10 features the flow f_{new} instead of f. As it can be verified on the VBG, both are related by the simple change of variables $f = f_{new} - f_{IA}$.
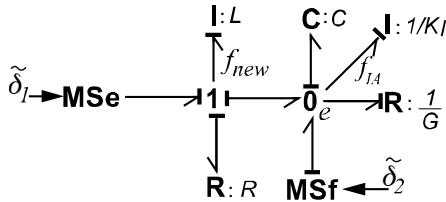

Figure 10: Closed-loop with IA and perturbations.

The addition of the integral action on e modifies the desired dynamics proposed in the original TBG of Figure 2b. This will have an impact in the dynamic response of the closed-loop system as shown by the simulations results of the next subsection. However, the asymptotic stability is conserved, what is demonstrated next.

Stability Analysis of the closed loop with IA: The EP of the new closed-loop system can be computed directly from the BG of Figure 10 by following the procedure detailed in (Breedveld 1984), see also (Junco 1993), i.e. making zero the incoming power variables of the storage elements in integral causality and reading through the causal paths and the constitutive

relationships of the elements. For constant $\tilde{\delta}_1$ and $\tilde{\delta}_2$ the EP is $e = 0$, $f_{new} = \tilde{\delta}_1/R$ and $f_{IA} = \tilde{\delta}_1/R + \tilde{\delta}_2$.

The stability of the EP can be analyzed from Figure 10 ignoring the sources (as all the elements are linear, this is the incremental BG around the EP). The rationale is roughly sketched next, for details about the procedure see the propositions stated in Junco (2001a). The total energy V in the storage elements is a positive definite function of the states: $V(e, \Delta f_{new}, \Delta f_{IA}) > 0$, where Δ denotes the deviation of the corresponding variable off the EP. Then, it can be naturally chosen as a candidate Lyapunov function. Its orbital derivative $\dot{V}$ is just the power into the storages, which equals minus the power into the dissipators. With all the storage elements in integral causality (thus, each of them providing a state variable) and all the R elements being strictly dissipative, $\dot{V}$ is a negative function of the states appearing in its argument, but not a negative-definite function of the states, as it does not depend on the three states but only on two of them: the BG of Figure 10 shows that the storage element that performs the IA does not impose causality on any R element, so that f_{IA} does not appear as an argument in $\dot{V}$. This implies that $\dot{V}$ is just a *negative semi-definite function* of the states, a property enough to assure the Lyapunov-stability of the EP. But a simple application of La Salle principle allows to conclude on the asymptotic stability of the EP.

3.2. Simulation results with integral action.

The experiment used in this section to compare the performance of the control laws with and without integral action is the following:

Experiment 2: the system starts with zero initial conditions and the voltage reference set in $V = 18V$, later, at time $t = 0.1s$ the voltage reference changes to $V = 16.7V$, then at time $t = 0.2s$ a constant current perturbation $\tilde{\delta}_2 = -0.4A$ at the load is applied. The parameter associated to the integral action is set at $K_I = 50$. Figures 11 and 12 show the simulation responses of *Experiment 2* with $R_L = 24\Omega$ and $E = 19.98V$ respectively.
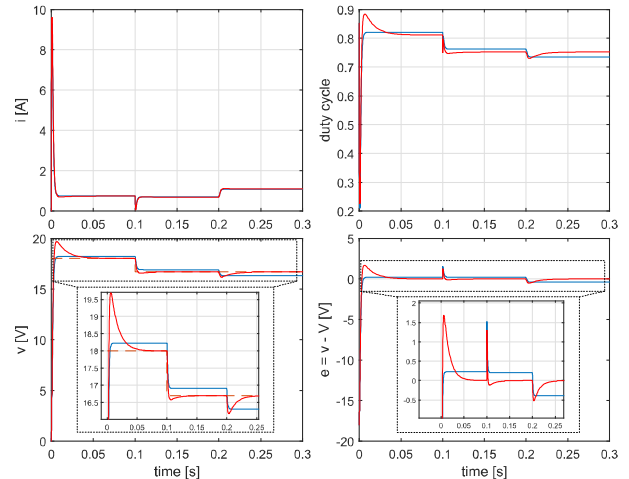

Figure 11: Simulation response with $R_L = 24\Omega$. In red with integral action, in blue without integral action.
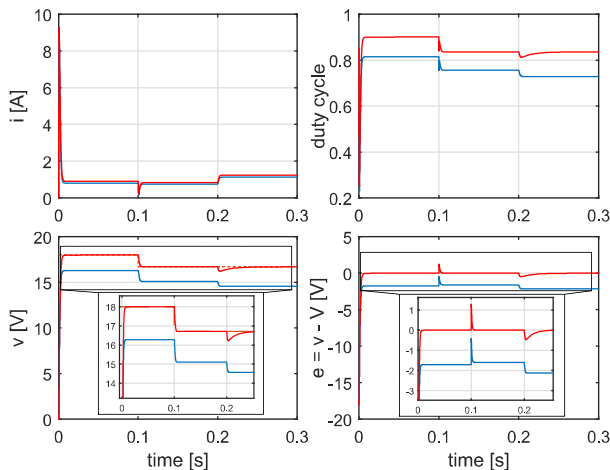
Figure 12: Simulation response with $E = 19.98V$. In red with integral action, in blue without integral action.

The simulations show that the integral action asymptotically rejects in both cases the perturbations induced by the parameter dispersion and the external disturbance.

4. CONCLUSIONS

This paper presented the synthesis, fully performed in the Bond Graph domain, of a nonlinear static-feedback controller globally stabilizing an arbitrary equilibrium point of a buck converter. The method has two steps: first, designing an exact model knowledge controller and, second, robustifying it with a disturbance rejecting outer control loop based on the addition of integral action. The whole design process has been discussed in detail in order to provide a methodological paradigm for its possible extension to other power electronic converters, or to any other kind of physical plant described by a Bond Graph or PHS model.

Starting from a Bond Graph and designing a controller forcing the closed-loop behaviour to emulate another Bond Graph, the first step is shown to be comparable to the Simultaneous Energy Shaping and Damping Assignment Passivity Based Control technique developed on Port-Hamiltonian Systems. The second step was executed with a method designed on purpose to conserve the PHS structure under the integral action addition. This kind of robustification however is prone to distort the type of evolution set as an objective when designing the exact model controller. This gives rise to the interest in investigating other ways of providing robustness against parameter uncertainty, unmodelled dynamics and external disturbances, among them the exploitation of the Diagnostic Bond Graph technique for control system design purposes.

Further work includes extending the results to other kind of loads of interest, possibly dynamic and/or non passive loads, as well as applying the methodology to other topologies of power electronic DC-DC converter. In view of the controller practical implementation, testing and tuning the closed-loop performance on a hybrid model where the control input is provided by a switch driven by a PWM-modulated continuous duty cycle is also planned, as well as performing the experimental validation of the controllers on a laboratory facility.

REFERENCES

Bacha S., Munteanu I., Bratcu A., 2014. Power Electronic Converters Modeling and Control: with Case Studies. London: Springer

Batlle C., Dòria-Cerezo A., Espinosa-Pérez G., Ortega R., 2009. Simultaneous interconnection and damping assignment passivity-based control: the induction machine case study. International Journal of Control, Volume 82, Issue 2: pp. 241-255.

Breedveld, P.C. 1984. 'A bond graph algorithm to determine the equilibrium state of a system', Journal of the Franklin Institute, Vol. 318, No. 2,. pp.71–75, ISSN 0016-0032.

Choudhury S., 2005. Designing a TMS320F280x Based Digitally Controlled DC-DC Switching Power Supply. TI App. Rep. SPRAAB3. Available from: http://www.ti.com/lit/an/spraab3/spraab3.pdf [accessed 15 May 2016]

Donaire, A. and Junco, S., 2009a. Energy Shaping, Interconnection and Damping Assignment, and Integral Control in the Bond Graph Domain, Simulation Modelling Practice and Theory, 17 (1), pp. 152-174.

Donaire, A. and Junco, S., 2009b. On the Addition of Integral Action to Port-Controlled Hamiltonian Systems, Automatica, 45 (8), pp. 1910-1916.

Dong Tan F., 2013. Address from the Editor-In-Chief of the IEEE J. Emerging & Selected Topics in Power Electronics. Available from: http://www.ieee-pels.org/publications/jstpe [accessed 15 May 2016]

Junco, S. 1993 'Stability analysis and stabilizing control synthesis via Lyapunov's second method directly on bond graphs on nonlinear systems', Proceedings of IECON'93, Maui, HII, 17–20 November, pp.2065–2069.

Junco, S. 2001a 'Lyapunov second method and feedback stabilization directly on bond graphs', Proc. ICBGM'2001, SCS-Simulation Series, Vol. 33, No. 1, pp.137–142.

Junco, S., 2001b. A Bond Graph Approach to Control System Synthesis. Proc. Int. Conf. on Bond Graph Modeling and Simulation, ICBGM 2001, SCS, Simulation Series, 33:1, ISBN: 1-56555-221-0. Pp. 125-130. January 7-11, Phoenix, Arizona, USA

Junco, S., 2004. Virtual Prototyping of Bond Graphs Models for Controller Synthesis through Energy and Power Shaping. Proc. The International

Conference on Integrated Modeling & Analysis in Applied Control & Automation,; Proc. IMAACA '2004, part of I3M 2004: International Mediterranean Modeling Multiconference, Vol. 2, pp. 100-109, October 28-31, Genoa, Italy

Karnopp, D. C., Margolis D. L., Rosenberg R. C. 2012. System dynamics: modeling, simulation, and control of mechatronic systems. John Wiley & Sons

Khalil, H., 2002. Nonlinear Systems Second Edition. New Jersey: Prentice-Hall.

Kwasinski, A., Krein, P. T., 2007. Passivity-based control of buck converters with constant-power loads. Power Electronics Specialists Conference, PESC 2007. IEEE, pp. 259-265, 17-21 June 2007, Orlando, FL.

Mohan, N. Undeland, T. Robbins, W., 1995. Power Electronics: converters, applications and design. John Wiley & Sons

Ortega R., van der Schaft A., Maschke B., Escobar G., 2002. Interconnection and damping assignment passivity-based control of port-controlled Hamiltonian systems. Automatica, Volume 38, Issue 4: pp. 585–596.

Ortega R., García-Canseco E., 2004. Interconnection and Damping Assignment Passivity-Based Control: A survey. European Journal of Control, 10, pp 432-450.

Sira-Ramírez H., Silva-Ortigoza R., 2006. Control Design Techniques in Power Electronics Devices. London: Springer-Verlag

Tan S. C., Lai Y. M, Tse, C. K., Cheung, M. K. H., 2006. Adaptive feedforward and feedback control schemes for sliding mode controlled power converters. IEEE Trans. Power Electron., vol. 21: no. 1, pp. 182–192

AUTHORS BIOGRAPHIES

Sergio Junco received the Electrical Engineer degree from the *Universidad Nacional de Rosario* (UNR) in 1976. In 1982, after 3 years in the steel industry and a 2-year academic stage at the University of Hannover, Germany, he joined the academic staff of UNR, where he currently is a Full-time Professor of System Dynamics and Control and Head of the Automation and Control Systems Laboratory. His current research interests are in modeling, simulation, control and diagnosis of dynamic systems, with applications in the fields of motion control systems with electrical drives, power electronics, mechatronics, vehicle dynamics and smart grids. He has developed, and currently teaches, several courses at both undergraduate and graduate level on System Dynamics, Bond Graph Modeling and Simulation, Advanced Nonlinear Dynamics and Control of Electrical Drives, as well as Linear and Nonlinear Control with Geometric Tools.

Juan Tomassini was born in Rosario, Argentina. He received his degree in Electrical Engineering from the Universidad Nacional de Rosario (UNR), Argentina, in 2013. He worked as an electrical generation programmer in the administrator company of the wholesale electricity market (CAMMESA). Since September 2014 he has been a PhD student in Electrical Engineering and Control at the Faculty of Engineering (FCEIA) of UNR. His work is supported by the Nacional Agency for Scientific and Technological Promotion (ANPCyT). His main research interests are on IDA-PBC, renewable energy and smart grids.

Matías A. Nacusse was born in Rosario, Argentina. He received the degree in Electronic Engineering from the Universidad Nacional de Rosario (UNR), Argentina, in 2007. Since April 2008 he has been a Ph.D. student in Electronic Engineering and Control at the Faculty of Engineering (FCEIA) of UNR under the supervision of Prof. S. Junco and Prof. M. Romero. He is a teaching assistant in two undergraduate courses, one on System Dynamics and Control and the other on Control of Electrical Drives, both at FCEIA-UNR. His main research interests are on Bond Graphs, Fault Tolerant Control and Nonlinear Control.